

DNA lesions proximity modulates damage tolerance pathways

Élodie Chrabaszczy¹, Luisa Laureti¹, Vincent Pagès^{1*}

¹Team DNA Damage and Genome Instability, Cancer Research Center of Marseille, CRCM, Aix Marseille univ, CNRS, inserm, institut Paoli-Calmettes, 13009 Marseille, France

*Correspondence to: vincent.pages@inserm.fr

Abstract:

The genome of all organisms is constantly threatened by numerous agents that cause DNA damages. When the replication fork encounters an unrepaired DNA lesion, two DNA damage tolerance pathways are possible: error-prone translesion synthesis (TLS) that requires specialized DNA polymerases, and error-free Damage Avoidance (DA) that relies on homologous recombination. The balance between these two mechanisms is essential since it defines the level of mutagenesis during lesion bypass, allowing genetic variability and adaptation to the environment, but also introducing the risk of generating genome instability. Here we report that the mere proximity of replication-blocking lesions located in opposite strands of the bacterial genome leads to a strong increase in the use of the error-prone TLS. This increase is caused by the local inhibition of homologous recombination due to the overlapping of single-stranded DNA regions generated downstream the lesions, and appears as a way for cells to respond to genotoxic stress by favoring the potentially mutagenic translesion synthesis pathway. We show that this response is independent of SOS activation, but that its mutagenic effect is additive with the one of SOS induction. Hence, the combination of SOS induction and lesions proximity leads to strong increase in the use of TLS that becomes the main lesion tolerance pathway used by the cell.

Introduction:

When replicating its genome, a cell may be facing unrepaired DNA lesions that need to be bypassed in order to achieve chromosomal replication. For this purpose, cells have evolved two DNA Damage Tolerance (DDT) pathways: i) Translesion Synthesis (TLS) by which specialized DNA polymerases insert a nucleotide directly opposite the lesion with the risk of introducing a mutation (1); ii) Homology Directed Gap Repair (HDGR) (2) by which the single-stranded DNA gap left downstream the lesion after a repriming event (3), is filled by homologous recombination (4, 5). In physiological conditions, upon encounter with a single blocking lesion, TLS represents a minor pathway, while Damage Avoidance events (including HDGR and damaged chromatid loss) accounted for most of the survival (2, 6). This partition between DDT pathways can be modulated by genetic factors. For instance, during a genotoxic stress, the induction

of the SOS system leads to an increase in the expression level of specialized DNA polymerases favoring TLS over HDGR (7). Also, when the homologous recombination machinery is impaired, the decrease in HDGR is accompanied by an increase in TLS (8). Besides the modulation of the actors of both pathways, either natural (SOS induction) or artificial (genes deletions or mutations), could a naturally occurring perturbation in the structure of the replication fork affect the partition in lesion tolerance? In this work we raised the question of what happens to the replication fork structure when lesions are present in opposite strands (an event occurring frequently during a genotoxic stress), and showed this event affects lesion tolerance by preventing HR and favoring TLS.

Results:

Lesion proximity increases TLS

In order to study the impact of lesions proximity on DDT pathways, we constructed integrating vectors that harbor one AAF (N2-AcetylAminoFluorene) lesion in each strand. These vectors were introduced at a specific locus in the chromosome of a living bacteria using a recently developed system that allows to monitor both TLS and HDGR at the damaged sites (6, 9). We initially chose a distance of 1.8kb to separate the two lesions in order to mimic a

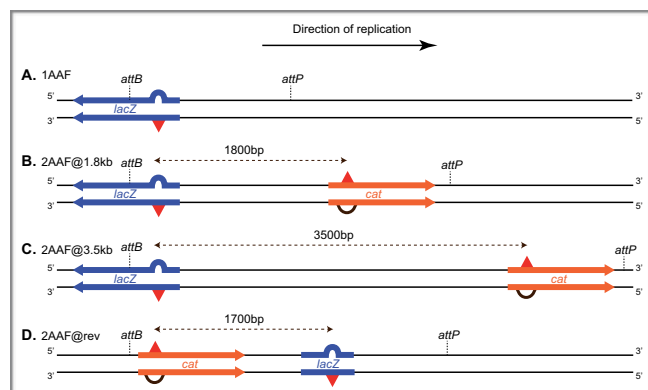


Figure 1: Map of the lesions once integrated in the bacterial genome between phage lambda *attB* and *attP* recombination sites. A: a single AAF lesion in the *lacZ* gene. B and C: 2 lesions are separated by 1.8 and 3.5kb. The first lesion encountered by the replication fork is located on the leading strand (*lacZ* gene) while the second lesion encountered is on the lagging strand (*cat* gene). D: reverse configuration where the lesions are separated by 1.7kb, the first lesion encountered by the replication fork is located on the lagging strand while the second lesion is on the leading strand.

realistic genotoxic stress. Indeed, such density of one lesion every 1.8kb corresponds to ~2500 lesions per chromosome which is equivalent to a UV irradiation of ~50J.m⁻² (10, 11). In our original vector design, the AAF lesion was located in the *lacZ* reporter gene (figure 1A). We kept this lesion in the same locus and added the second lesion in the chloramphenicol resistance gene (*cat*) on the opposite strand (figure 1B). Both AAF lesions are located in the *NarI* mutation hotspot where Pol V mediates error-free TLS (TLS0) and Pol II mediates -2 frameshift TLS (TLS-2) (12). A 3-nucleotide loop opposite to each lesion allows to monitor HDGR events.

TLS at *lacZ* site in the parental strain

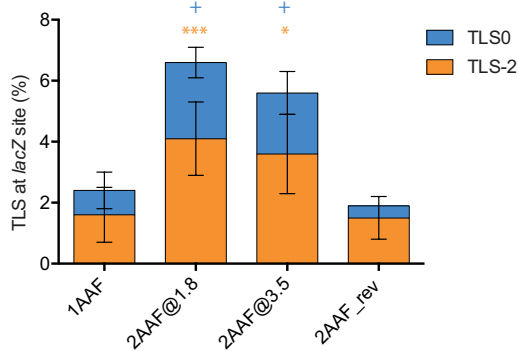
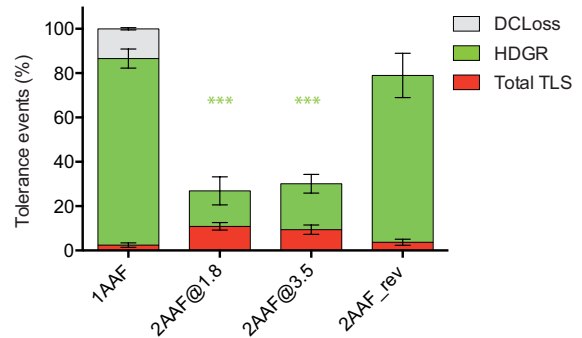


Figure 2: TLS events at the original *lacZ* locus in the parental strain (*uvrA mutS*) for the different lesions configuration. Pol V TLS is error-free (TLS0), while Pol II TLS leads to a -2 frameshift (TLS-2). The data represent the average and standard deviation of at least 3 independent experiments. Unpaired t-test was performed to compare TLS values from the integration of 2 lesions to the integration of a single lesion. *P<0.05; **P<0.005; ***P>0.0005

When monitoring TLS (figure 2) we observe that the presence of a second lesion at a distance of 1.8kb, strongly increases TLS at the original (*lacZ*) lesion site. We indeed observe a 3 fold increase in Pol V TLS, and a 2.5 fold increase in Pol II TLS (figure 2). Concomitant with this increase in TLS, we observe a strong decrease in survival (figure 3A). A single lesion doesn't induce any toxicity and is mostly tolerated by HDGR, while damaged chromatid loss accounts for a small fraction and TLS is a minor event representing ~2% of the surviving cells. The presence of the second lesion appears to be highly toxic for the cell since the viability drops to ~25%. The massive loss of viability is due partly to the fact that damaged chromatid loss is no longer possible since both chromatids are damaged, but mostly to a strong decrease in HDGR. We hypothesized that this inhibition of HDGR was caused by the overlapping of daughter strand gaps generated at the opposite lesions (figure 5B). This would suggest that repriming on the leading strand had occurred mostly beyond 1.8kb downstream the lesion, and that the Okazaki fragment preceding the lesion had initiated before 1.8kb (figure 4B). In this situation, no dsDNA substrate is available opposite any of the lesions to allow RecA nucleofilament invasion (D-loop) that is the initial step of HDGR (13, 14). This strong decrease in HDGR is leading to the observed increase in TLS (Figure 2). This is consistent with our previous

A. Lesion tolerance in the parental strain



B. Lesion tolerance in a $\Delta recJ$ strain

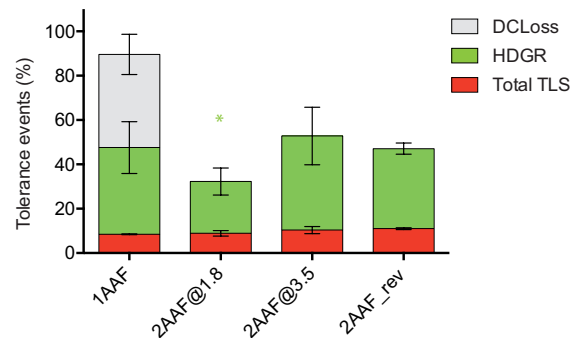


Figure 3: Partitioning of the events allowing the cell to survive the damages in the parental strain (A) and in the $\Delta recJ$ strain (B). Tolerance events (Y axis) represent the percentage of cells able to survive in presence of the integrated lesion(s) compared to the lesion-free control. Total TLS (or HDGR) represents the percentage of cells that achieved TLS (or HDGR) at the *lacZ* site and/or at the *cat* site when present. Damaged chromatid loss is only observed for the single lesion construct.

The data represent the average and standard deviation of at least 3 independent experiments. Unpaired t-test was performed to compare HDGR values from the integration of 2 lesions to the integration of a single lesion. *P<0.05; **P<0.005; ***P>0.0005

observation that TLS increased when HR was impaired genetically by mutations in *recA* or inactivation of *recF* or *recO* (8). Because of the combined increase in TLS and decrease in HDGR, total TLS events (including TLS at both AAF sites) represent now more than 40% of the surviving cells (as compared to 2% for a single lesion).

5' end resection by RecJ prevents HDGR

We then reasoned that by increasing the distance between the two lesions, we should avoid this overlap of daughter strand gaps and restore some viability. We constructed and integrated a new vector where both AAF lesions are now 3.5kb apart (Figure 1C). Compared to the previous situation where lesions were 1.8kb apart, neither TLS (figure 2) nor HDGR or survival (figure 3A) were significantly different. It appears therefore that even at 3.5kb, the gaps generated at the lesion are still overlapping, inhibiting HDGR and favoring TLS. It is unlikely that repriming events on the leading strand would occur beyond 3.5kb, since the gaps observed after UV irradiation have been estimated to be in the range of ~1-2kb (15). Similarly, on the lagging strand, Okazaki fragments

are expected to be shorter than 3kb (16). Therefore, both in the leading and lagging strand, one can expect dsDNA on the strand opposing the lesion, and HR should be observed. Since we didn't observe any recovery in HDGR when lesions are 3.5kb apart, we hypothesize that the 5' end of the reprimed fragment or of the Okazaki fragment preceding the lesion could be resected by a 5'3' exonuclease, creating overlapping ssDNA regions that would prevent HDGR.

Daughter strand gaps repair occurs through the RecF pathway where RecFOR mediates the loading of RecA protein onto SSB-coated ssDNA (17). Belonging to the RecF pathway, RecQ helicase and RecJ nuclease participate to the process by widening the gaps (18, 19). RecJ exonuclease possesses a 5'3' polarity (20) that combined with the action of RecQ helicase can resect the newly synthesized DNA that had reprimed downstream the lesion. Consistent with this role of RecJ, following the introduction of a single G-AAF lesion, the inactivation of *recJ* (comparison of 1AAF between figure 3A and figure 3B) leads to a strong decrease in HDGR that is mostly compensated by damaged chromatid loss events, and also accompanied by an increase in TLS as previously observed for *recF* or *recO* mutants (8). When a second lesion is present at 1.8kb, *recJ* inactivation has no effect on the repartition of DDT events. However, when a second lesion is present at 3.5kb, *recJ* inactivation restores some viability by increasing HDGR (compare 2AAF@3.5 between figure 3A and 3B) to the level observed with a single lesion. This result supports our model where HDGR is prevented by the overlapping of opposite daughter strand gaps. In the presence of RecJ exonuclease, gaps are extended beyond 3.5kb causing the ssDNA-gaps to overlap and preventing HDGR to occur. In the absence of RecJ, repriming events that occur before 3.5kb are not resected and allow HDGR (figure 5C). This observation with only 2 DNA lesions artificially introduced on the genome would imply that RecJ has opposite effects depending on the density of lesions. At low lesion density, DNA resection by RecJ would expand the gaps and increase the efficiency of HDGR, whereas at high lesion density, the gaps expansion would lead to their overlapping that would prevent HDGR. That is indeed what has been observed by Courcelle *et al.* who compared UV-survival of a *recJ* to a WT strain (21): at low doses, the *recJ* strain is more sensitive than the WT strain showing the requirement of RecJ for HDGR. At higher doses, the *recJ* strain becomes more resistant than the WT strain showing the deleterious effect of RecJ when lesion density is higher. Interestingly, the UV dose where the effect of RecJ switches is in the range of 60J.m⁻² which correspond to a lesion density that is in the same range as our experimental setup.

The decrease in HDGR observed in the *recJ* strain in the presence of a single AAF lesion supports the model by which RecJ widens the ssDNA gaps generated downstream a DNA lesion. Interestingly, while RecJ has been mostly described as acting at the 5' terminus of an Okazaki fragment on the lagging strand (22), we observe the same effect whether the lesion is located on the lagging or on the leading

Lesion tolerance in a $\Delta recJ$ strain

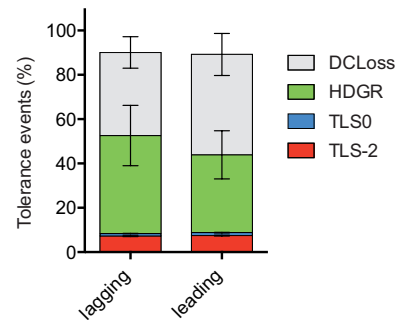


Figure 4: Partitioning of the DTT events in the presence of one single AAF lesion inserted in the *recJ* deficient strains. The lesion has been inserted in either the leading or the lagging strand of *E. coli* chromosome. Tolerance events (Y axis) represent the percentage of cells able to survive in presence of the integrated lesion compared to the lesion-free control. The data represent the average and standard deviation of at least three independent experiments. No significant difference is observed in the level of HDGR whether the lesion is inserted on the lagging or leading strand. The data represent the average and standard deviation of at least 3 independent experiments. Unpaired t-test was performed to compare values from the integration of 2 lesions to the integration of a single lesion. *P<0.05; **P<0.005; ***P>0.0005

strand (figure 4), indicating that RecJ can act with similar efficiency both at a repriming event that occurred on the leading strand, and at an Okazaki fragment on the lagging strand.

The initial gap generated downstream the lesion is in the range of 1.8 to 3.5kb

It is interesting also to note that in the *recJ* strain (figure 3B), the survival is much lower with 2 lesions since damaged chromatid loss that accounted for ~50% of survival with a single lesion is no longer possible (both chromatids being damaged). However, the level of HDGR is similar when 2 lesions are 3.5kb apart and when one lesion is isolated. This suggests that in the absence of resection ($\Delta recJ$), the amount of ssDNA downstream the lesions is similar in both situations, and therefore that the gap formed downstream a single lesion is shorter than 3.5kb (before resection). Together with the previous observation that HDGR is strongly inhibited when the lesions are 1.8kb apart (whether RecJ is present or not), we can conclude that the gap generated downstream a lesion is in the range of 1.8 to 3.5kb. This size of gap (in the absence of expansion by RecJ) seems insufficient to promote efficient homologous recombination since *recJ* deletion leads to a strong decrease in HDGR at a single lesion. Further studies will be required in order to determine how far the gap is extended by RecJ in order to achieve WT-levels of HDGR.

Daughter strand gaps overlapping prevents HDGR

To further challenge our model, we constructed a vector with two lesions in a reverse configuration where the first lesion encountered by the replication fork is located in the lagging strand, and the second

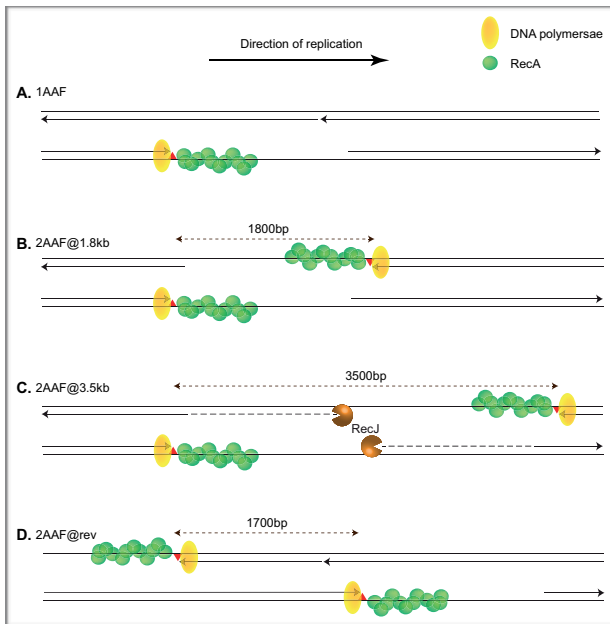


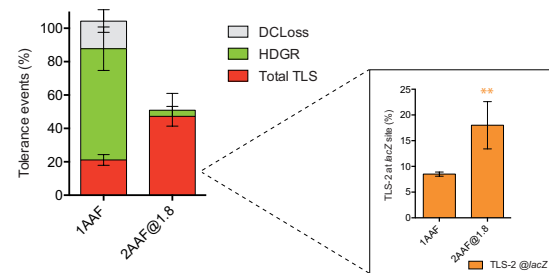
Figure 5: Structure of the region of damaged DNA that is replicated. A: when one single lesion is encountered on the leading strand, repriming occurs downstream the lesion. The gap can be filled by HDGR or TLS. B: when 2 lesions distant from 1.8kb are present on opposite strands, the two ssDNA regions generated on opposite strands prevent HDGR and favor TLS. C: when the 2 lesions are separated by 3.5kb, 5'-end resection by RecJ leads to overlapping ssDNA gaps that prevent HDGR and favor TLS. In the absence of RecJ, ssDNA gaps are no longer overlapping and HDGR is possible. D: in the reverse configuration, when the first lesion encountered by the replication fork is located on the lagging strand, no overlapping daughter strand gaps occurs and HDGR level is similar to the one of a single lesion.

lesion, positioned 1.7kb downstream is located in the leading strand (figure 1D). In this configuration, no matter how far the repriming occurs, nor if gap widening occurs, the ssDNA gaps generated downstream each lesion are not overlapping and therefore, one does not expect HDGR inhibition (Figure 5D). Integration of this vector indeed shows a high level of HDGR similar to the one observed with a single lesion, despite the proximity of the two lesions (figure 3A). In addition, the TLS level at the initial *lacZ* locus is not increased by the proximity of the second lesion (figure 2). This observation rules out the possibility that the increase in TLS observed with the constructions 2AAF@1.8 and 2AAF@3.5 was due to SOS induction by the additional lesion, and confirms our hypothesis that TLS increase is the result of HDGR inhibition by overlapping ssDNA gaps.

Discussion:

In conclusion, we show here a model where the mere proximity of DNA lesions leads to a structural inhibition of homologous recombination that in turn favors Translesion synthesis. This increase in TLS is independent of SOS activation or of any modulation of genetic factors. Such a constrain due to the proximity of DNA lesions may occur naturally and quite frequently during a genotoxic stress, and allows cells to modulate their DNA damage response by favoring TLS. Strong genotoxic stresses are also

A. Lesion tolerance in a LexA(Def) strain



B. Lesion tolerance in a NER proficient strain

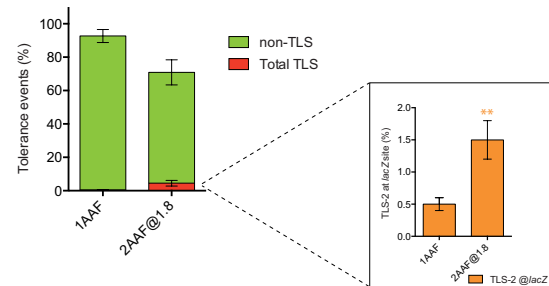


Figure 6: Partitioning of DDT pathways at one single AAF lesion and at 2 AAF lesions on opposite strands at 1.8kb distance A: in a LexA(Def) strain where the SOS system is constitutively induced. B: in a strain proficient for Nucleotide Excision Repair (*uvrA+*). The inserts represent Pol II mediated TLS-2 at the *lacZ* site only, to allow direct comparison of mutagenic TLS between one and two lesions. The data represent the average and standard deviation of at least 3 independent experiments. Unpaired t-test was performed to compare TLS values from the integration of 2 lesions to the integration of a single lesion. *P<0.05; **P<0.005; ***P>0.0005

known for inducing the SOS response that also favors TLS by increasing the expression of specialized polymerases. By introducing one or 2 lesions in a LexA deficient strain where the SOS system is constitutively induced, we show that the two mechanisms are indeed additive (figure 6A): the SOS induction leads to a ~5 fold increase in the use of the TLS pathway, and the proximity of the DNA lesions leads to an additional ~2 fold increase in the use of TLS. Overall, error-prone TLS accounts for ~90% of survival when lesions are close by and SOS is induced.

Finally, in order to extrapolate this observation to a wild-type context where lesions can be repaired, we introduced the lesions in the genome of a Nucleotide Excision Repair proficient (NER+) strain (figure 6B). The level of TLS at a single AAF is much lower in the NER+ strain compared to the NER- strain (figure 2) due to the fact that the lesion is frequently repaired before TLS could occur. When integrating two lesions, we observe a strong recovery in the survival in the NER+ compared to the NER- strain, that is mostly due to repair (that cannot be distinguish from HDGR in our system). Despite this high level of repair, the structural effect due to the lesions proximity at unrepaired lesions persists and leads to a strong increase in TLS compared to the single lesion.

Methods

Plasmid construction

Vector harboring a single lesion or dual lesions are constructed using the gap-duplex method as previously described (23, 24). Table S1 shows all the plasmids used in this study.

pEC29 and pEC30 are derived from previously described plasmids pVP143 and pVP144 (6). The chloramphenicol resistance gene (*cat*) and its promoter have been added in the opposite orientation with respect to the *lacZ* gene, in order to serve as a reporter gene where is introduced the second lesion. The 5' end of the *cat* gene has been modified by site directed mutagenesis in order to allow insertion of the AAF-modified oligonucleotide (plasmid pEC30) and the Nar+3 strand marker on the opposite strand (pEC29).

pEC37 and pEC38 are modified versions of pEC29 and pEC30 where a 1.7kb spacer (mCherry and GFP genes without their promoter) have been inserted between the two reporter genes (*lacZ* and *cat*) in order to increase the distance between the two lesions.

pEC45 and pEC46 are modified versions of pEC29 and pEC30 where the *cat* gene was cloned on the other side of *lacZ* gene regarding the attL integration site. A transcription termination site was added between *lacZ* and *cat* genes to avoid any potential interference between transcription and DDT events at the *cat* lesion. The integration of the pEC45/pEC46 duplex doesn't reconstitute a functional *lacZ* gene (see Figure 1), so TLS events are monitored by sequencing.

All six vectors contain the following characteristics: the R6K replication origin that allows the plasmid replication only if the recipient strain contains the *pir* gene, the ampicillin resistance gene that allows selection of integrated colonies, the chloramphenicol resistance gene as reporter for TLS at one lesion, and the 5' end of the *lacZ* gene in fusion with the attL recombination site of phage lambda. The P'3 site of attL has been mutated (AATCATTAT to AATTATTAT) to avoid the excision of the plasmid once integrated. These vectors are produced in strain EC100D *pir*-116 (from Epicentre Biotechnologies - *cat*# EC6P0950H) in which the *pir*-116 allele supports higher copy number of R6K origin plasmids.

Strains

All strains are derived from FBG151 and FBG152 (25). After integration of the vector in the attR site, the lesion at the *lacZ* site is located on the lagging strand in FBG151 and its derived strains, and on the leading strand in FBG152 and its derived strains. Gene disruptions were achieved by the one-step PCR method (26). The following FBG151 and FBG152 derived strains were constructed by P1 transduction (Table S2).

Monitoring DDT events

Competent cells preparation and integration of lesion-containing vectors were conducted as previously described (6, 24). Briefly, a non-damaged control vector and the lesion(s) containing vector are transformed together with an internal standard plasmid (pVP146) in electrocompetent cells

expressing the *int-xis* gene of phage lambda. After a 45 minutes incubation period, cells are plated on LB agar media containing antibiotic and X-gal indicator. Survival is calculated by the ratio of colonies resulting from the integration of the damaged vector over the non-damaged control, corrected by the transformation efficiency of the internal standard plasmid (pVP146).

For the single lesion containing vectors, Pol V mediated TLS0 and Pol II mediated TLS-2 were measured by counting blue colonies after integration of pVP141/142 and pVP143/pVP144 duplexes respectively (6). HDGR and damaged chromatid loss was assessed by monitoring blue and white colonies after the integration of pLL1/pLL7 as previously described (2, 27).

For the dual lesions containing vectors pEC29/pEC30 and pEC37/pEC38, TLS-2 at *lacZ* site was measured as blue colonies on X-gal indicator plate and TLS-2 at *cat* site was measured as chloramphenicol resistant colonies. All events (including TLS-2) for these plasmids and for pEC45/pEC46 were monitored by Sanger sequencing after whole colony PCR amplification of the damaged region. Chromatogram analysis allows to visualize events that occurred on both strands of each damaged site (Fig. S1). Figure 2 represents all TLS events that occurred at the *lacZ* site regardless of what has happened at the other site. In figures 3A-B, "total TLS" represents the percentage of cells that survived using TLS at *lacZ* and/or at *Cm* site. HDGR represents the percentage of cells that survived using HDGR at *lacZ* and/or at *Cm* but didn't use TLS. Detail of the tolerance events at both sites are presented in table S3.

Integrations were performed in FBG151 and FBG152 derived strains allowing lesions at the *lacZ* site and at the *cat* site to be alternatively on the lagging or leading strand. Since no difference was observed for the 2 orientations, the graphs and table represent the average of integration events obtained in both orientations.

Author Contributions: VP designed the experiments. EC and LL carried out the experiments. EC, LL and VP analyzed the data. VP wrote the paper. All authors discussed the results and commented on the manuscript.

Acknowledgments: this work was supported by Agence Nationale de la recherche (ANR) Grant GenoBlock ANR-14-CE09-0010-01. We thank Mauro Modesti for critical reading of the manuscript.

References:

1. Pagès V, Fuchs RPP (2002) How DNA lesions are turned into mutations within cells? *Oncogene* 21(58):8957–8966.
2. Laureti L, Demol J, Fuchs RP, Pagès V (2015) Bacterial Proliferation: Keep Dividing and Don't Mind the Gap. *PLoS Genet* 11(12):e1005757.
3. Heller RC, Marians KJ (2006) Replication fork reactivation downstream of a blocked nascent leading strand. *Nature* 439(7076):557–562.

4. Kuzminov A (1999) Recombinational repair of DNA damage in *Escherichia coli* and bacteriophage lambda. *Microbiol Mol Biol Rev* 63(4):751–813.
5. Rice KP, Cox MM (2001) *Recombinational DNA Repair in Bacteria: Postreplication* (John Wiley & Sons, Ltd, Chichester) doi:10.1038/npg.els.0000689.
6. Pagès V, Mazon G, Naiman K, Philippin G, Fuchs RP (2012) Monitoring bypass of single replication-blocking lesions by damage avoidance in the *Escherichia coli* chromosome. *Nucleic Acids Res* 40(18):9036–9043.
7. Naiman K, Philippin G, Fuchs RP, Pagès V (2014) Chronology in lesion tolerance gives priority to genetic variability. *Proc Natl Acad Sci USA* 111(15):5526–5531.
8. Naiman K, Pagès V, Fuchs RP (2016) A defect in homologous recombination leads to increased translesion synthesis in *E. coli*. *Nucleic Acids Res* 44(16):7691–7699.
9. Pagès V, Fuchs RP (2017) Inserting site-specific DNA lesions into whole genomes. *Methods in Molecular Biology*.
10. Rupp WD, Howard-Flanders P (1968) Discontinuities in the DNA synthesized in an excision-defective strain of *Escherichia coli* following ultraviolet irradiation. *J Mol Biol* 31(2): 291–304.
11. Howard-Flanders P, Theriot L, Stedeford JB (1969) Some properties of excision-defective recombination-deficient mutants of *Escherichia coli* K-12. *J Bacteriol* 97(3):1134–1141.
12. Fuchs RP, Schwartz N, Daune MP (1981) Hot spots of frameshift mutations induced by the ultimate carcinogen N-acetoxy-N-2-acetylaminofluorene. *Nature* 294(5842):657–659.
13. Kowalczykowski SC, Dixon DA, Eggleston AK, Lauder SD, Rehrauer WM (1994) Biochemistry of homologous recombination in *Escherichia coli*. *Microbiol Rev* 58(3):401–465.
14. McEntee K, Weinstock GM, Lehman IR (1979) Initiation of general recombination catalyzed in vitro by the recA protein of *Escherichia coli*. *Proc Natl Acad Sci USA* 76(6):2615–2619.
15. Iyer VN, Rupp WD (1971) Usefulness of benzoylated naphthoylated DEAE-cellulose to distinguish and fractionate double-stranded DNA bearing different extents of single-stranded regions. *Biochim Biophys Acta* 228(1):117–126.
16. Okazaki R, Okazaki T, Sakabe K, Sugimoto K (1967) Mechanism of DNA replication possible discontinuity of DNA chain growth. *Jpn J Med Sci Biol* 20(3):255–260.
17. Morimatsu K, Kowalczykowski SC (2003) RecFOR proteins load RecA protein onto gapped DNA to accelerate DNA strand exchange: a universal step of recombinational repair. *Mol Cell* 11(5):1337–1347.
18. Xia J, et al. (2016) Holliday junction trap shows how cells use recombination and a junction-guardian role of RecQ helicase. *Sci Adv* 2(11):e1601605.
19. Viswanathan M, Lovett ST (1998) Single-strand DNA-specific exonucleases in *Escherichia coli*. Roles in repair and mutation avoidance. *Genetics* 149(1):7–16.
20. Lovett ST, Kolodner RD (1989) Identification and purification of a single-stranded-DNA-specific exonuclease encoded by the recJ gene of *Escherichia coli*. *Proc Natl Acad Sci USA* 86(8): 2627–2631.
21. Courcelle CT, Chow K-H, Casey A, Courcelle J (2006) Nascent DNA processing by RecJ favors lesion repair over translesion synthesis at arrested replication forks in *Escherichia coli*. *Proc Natl Acad Sci USA* 103(24):9154–9159.
22. Courcelle J, Hanawalt PC (1999) RecQ and RecJ process blocked replication forks prior to the resumption of replication in UV-irradiated *Escherichia coli*. *Mol Gen Genet* 262(3):543–551.
23. Koehl P, Burnouf D, Fuchs RP (1989) Construction of plasmids containing a unique acetylaminofluorene adduct located within a mutation hot spot: A new probe for frameshift mutagenesis. *J Mol Biol* 207(2):355–364.
24. Pagès V, Fuchs RP (2018) Inserting Site-Specific DNA Lesions into Whole Genomes. *Methods Mol Biol* 1672(Chapter 9):107–118.
25. Esnault E, Valens M, Espéli O, Boccard F (2007) Chromosome structuring limits genome plasticity in *Escherichia coli*. *PLoS Genet* 3(12):e226.
26. Datsenko KA, Wanner BL (2000) One-step inactivation of chromosomal genes in *Escherichia coli* K-12 using PCR products. *Proc Natl Acad Sci USA* 97(12):6640–6645.
27. Laureti L, Lee L, Philippin G, Pagès V (2017) A non-catalytic role of RecBCD in homology directed gap repair and translesion synthesis. *Nucleic Acids Res.* doi:10.1093/nar/gkx217.